S8. FACTORS OTHER THAN CLIMATE CHANGE, MAIN DRIVERS OF 2014/15 WATER SHORTAGE IN SOUTHEAST BRAZIL

Friederike E. L. Otto, Caio A. S. Coelho, Andrew King, Erin Coughlan de Perez, Yoshihide Wada, Geert Jan van Oldenborgh, Rein Haarsma, Karsten Haustein, Peter Uhe, Maarten van Aalst, Jose Antonio Aravequia, Waldenio Almeida, and Heidi Cullen

This document is a supplement to "Factors Other than Climate Change, Main Drivers of 2014/15 Water Shortage in Southeast Brazil," by Friederike E. L. Otto, Caio A. S. Coelho, Andrew King, Erin Coughlan de Perez, Yoshihide Wada, Geert Jan van Oldenborgh, Rein Haarsma, Karsten Haustein, Peter Uhe, Maarten van Aalst, Jose Antonio Aravequia, Waldenio Almeida, and Heidi Cullen (*Bull. Amer. Meteor. Soc.*, **96** (12), S35–S40) • DOI:10.1175/BAMS-D-15-00120.1

For method (ii) (see main text), because we do not know the exact pattern of anthropogenic warming to remove from the SSTs, 11 equally likely patterns of warming are obtained by calculating the difference between nonindustrial and present day simulations for available CMIP5 models (Taylor et al. 2012). We chose all those models from the CMIP5 archive that have at least three ensemble members in the nonindustrial simulations (CanESM2, CCSM4, CNRM-CM5, CSIRO-Mk3-6-0, GFDL-CM3, GISS-E2-H, GISS-E2-R, HadGEM2-ES, IPSL-CM5A-MR, IPSL-CM5A-LR, and MIROC-ESM). As a result there are 11 different initial conditions ensembles ("natural") representing the analogous year in the counterfactual experiment. These are forced with preindustrial atmospheric gas composition, the SSTs obtained by subtracting the CMIP5-estimates of the human influence on SST from the observed OSTIA SST values and the sea ice extent that correspond to the year of maximum sea ice extent in each hemisphere of the OSTIA record. The natural experiment has 7041 ensemble members, the climatology of the current climate has 3816 members and the current climate of 2014/15 has 1045 ensemble members.

For (iii) we chose a subset of the CMIP5 ensemble that adequately represented the variability of precipitation seen in the observed record. A Kolmogorov–Smirnov (KS) test was employed to determine whether the model simulations do represented the variability seen in the observational record used in Fig. 8.1 in the main text. To account for the high lag correlations in the observed time series the degrees of freedom used to determine the significance of the KS-statistic were reduced accordingly. Models were deemed to have passed this test if, firstly, at least three historical simulations were available for analysis, and, secondly, no more than one of the three (or more) historical simulations was significantly different ($p < 0.05$) from the observational time series. The following models passed the test: ACCESS1.3, bcc-csm1.1, CCSM4, CNRM-CM5, GFDL-CM3, GISS-E2-H, GISS-E2-R, HadGEM2-ES, and MRI-CGCM3.

In Fig. S8.1 we show trends of the factors that influence evaporation in the CMIP5 ensemble. Temperature rises, but downward solar radiation at the surface stays roughly the same and relative humidity and soil moisture decline on average. The latter indicates that the lack of moisture availability limits evaporation, so that the negative trend in precipitation seen in many models also causes a negative trend in evaporation, leading to negligible trends in $P-E$.

Figure S8.2 shows maps of the observed trends up to the present and the CMIP5 mean trend up to the present and into the future for precipitation and $P-E$. All of these show drying north of the study area and wetting to the south. However, the observed trends are much larger than the modelled trends, although still within the bandwidth of the CMIP5 ensemble (around 90%, see van Oldenborgh et al. 2013a). The

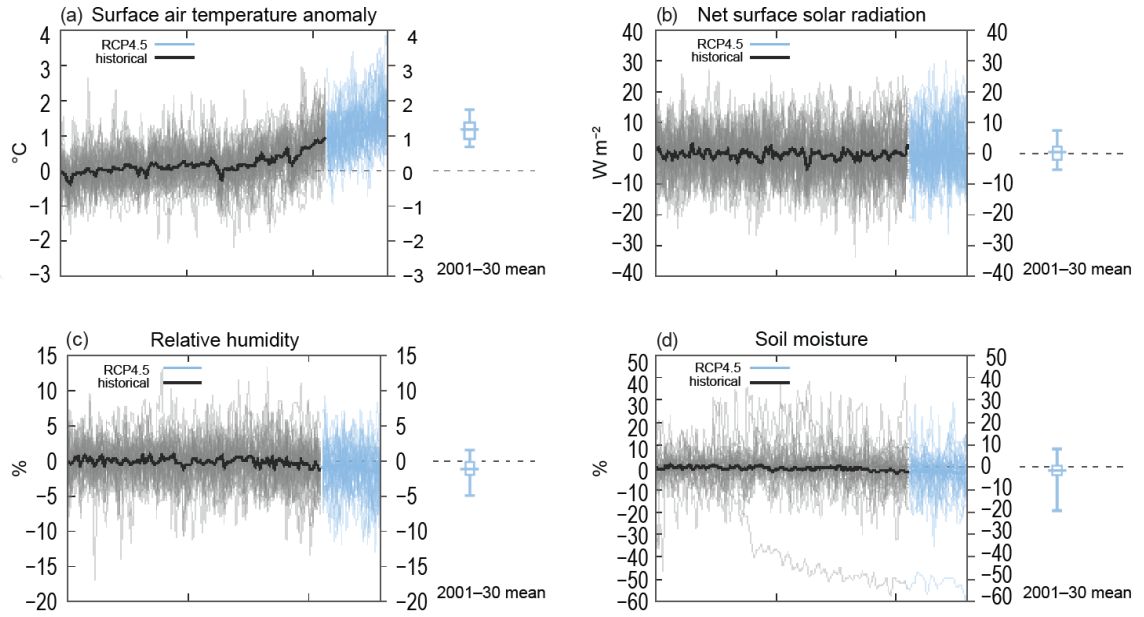

Fig. S8.1. Factors influencing evaporation. (a) Anomalous surface air temperature (°C) averaged over the São Paulo area (15°–20°S; 48°–40°W) simulated by CMIP5 models. The reference period is 1900–30. Black: historical runs, 1900–2005; blue: RCP4.5 extensions, 2006–30. (b) As in (a), but for net surface solar radiation (W m^{-2}). (c) As in (a) but for relative humidity (%). (d) As in (a) but for soil moisture (%). Thin lines represent one ensemble member per model, the thick black line the ensemble mean. The box-and-whisker diagram on the right side indicates the 5th, 25th, 50th, 75th, and 95th percentile of the distribution of the 2001–30 30-yr mean relative to the 1901–30 mean; this includes both the remaining natural variability and the model spread (van Oldenborgh et al. 2013b).

modelled trends are also small compared to the natural variability; the shading indicates regions where the trend does not exceed one standard deviation of the natural variability in the trend.

In Fig. S8.3 we show that in the precipitation trends up to the present, the natural variability dominates over the model spread. However, as trends in evaporation tend to cancel trends in precipitation, the $P-E$ natural variability is smaller and roughly equal to the model spread. For projections up to the end of the century the model differences dominate.

Figure S8.4 is similar to Fig. 8.2f in the main text but instead of contrasting the present (2006–22) with the world that might have been to highlight changes in drought hazard risk due to past anthropogenic greenhouse gas emissions here we look at changes due to past and future emissions. Even with the high forcing scenario RCP8.5 there is no clear signal of anthropogenic emissions increasing or decreasing the hazard analyzed in this study in the ensemble mean, although individual models do show increases and decreases.

REFERENCES

Taylor, K. E., R. J. Stouffer, and G. A. Meehl, 2012: An overview of CMIP5 and the experiment design. *Bull. Amer. Meteor. Soc.*, **93**, 485–498, doi:10.1175/BAMS-D-11-00094.1.

van Oldenborgh, G. J., F. J. Doblas-Reyes, S. S. Drijfhout, and E. Hawkins, 2013a: Reliability of regional model trends. *Environ. Res. Lett.*, **8**, 014055, doi:10.1088/1748-9326/8/1/014055.

——, G. J., M. Collins, J. Arblaster, J. H. Christensen, J. Marotzke, S. B. Power, M. Rummukainen, and T. Zhou, Eds., 2013b: Annex I: Atlas of global and regional climate projections.*Climate Change 2013: The Physical Science Basis*, T. F. Stocker et al., Eds., Cambridge University Press, 1311–1393.

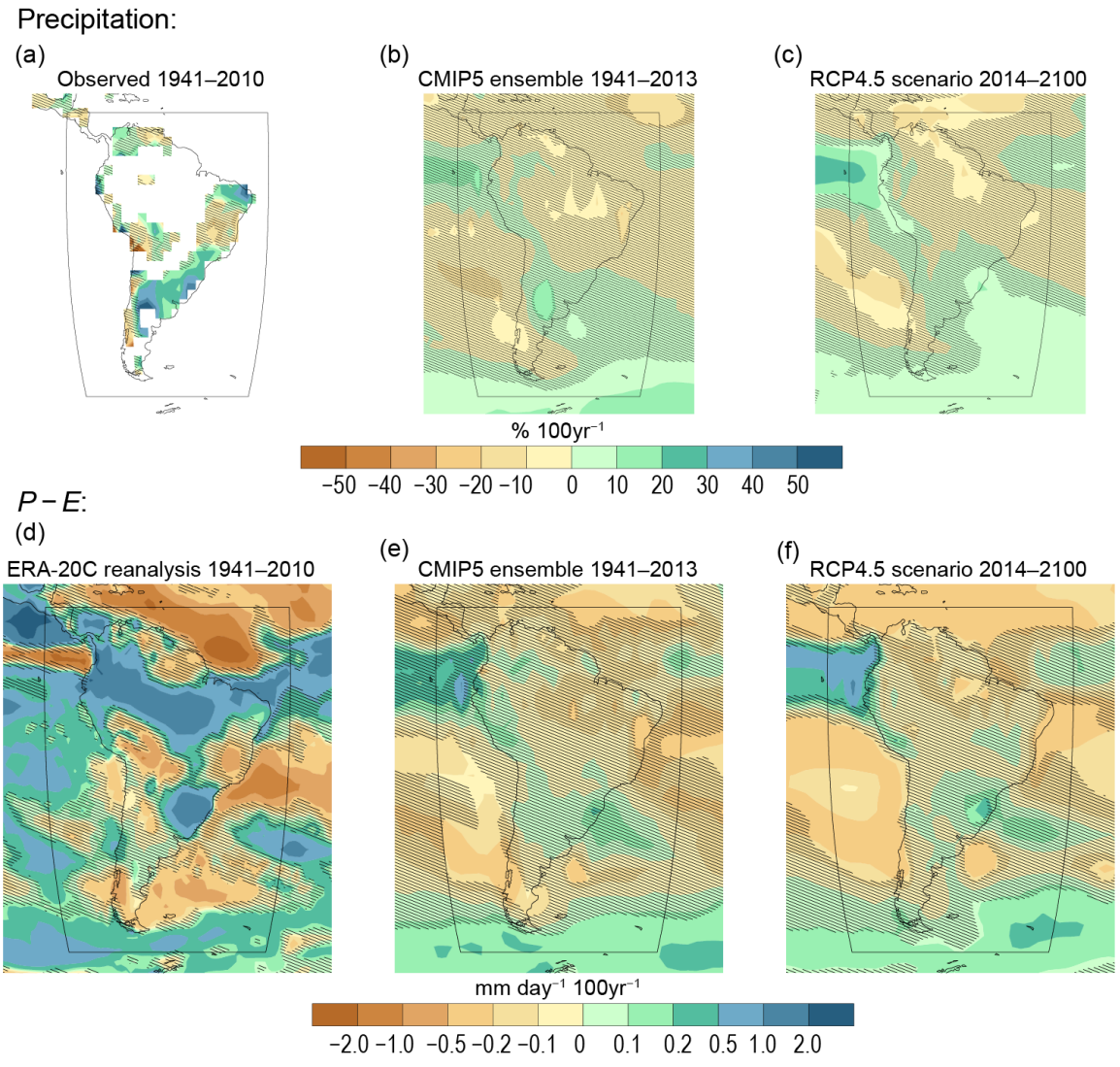

Fig. S8.2 (a) Observed linear trend in precipitation 1941–2010 in South America, the hatching denotes areas where the residuals of the linear trend fit are larger than the trend itself. (b) As in (a), but for the CMIP5 ensemble 1941–2013 used in van Oldenborgh et al. 2013b. (c) Projections 2014–2100 in the RCP4.5 scenario. (d)–(f) As in (a)–(c), but for *P* − *E*. As there are no observations for evaporation in (d) we used the ERA-20C reanalysis instead.

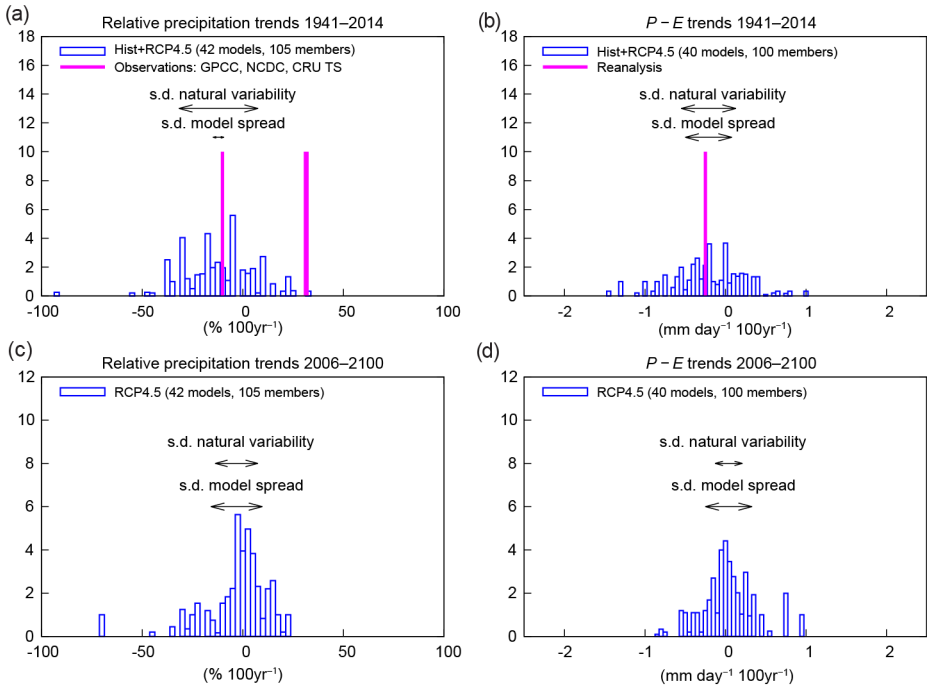

Fig. S8.3. Distribution of CMIP5 trends up to the present in (a) precipitation and (b) *P* − *E*. (c),(d) As in (a),(b), but for the projections.

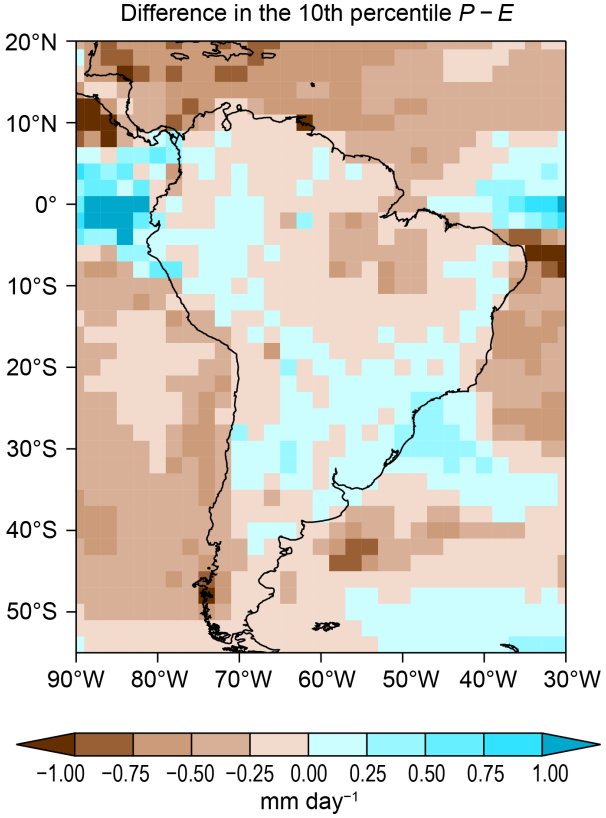

Fig. S8.4. Difference in mean *P* − *E* (mm day^{-1}) below the 10th percentile for RCP8.5 scenario (2080–99 minus 2006–22).